# A new approach to the prediction of temperature of the workpiece of face milling operations of Ti-6Al-4V

G.M. Pittalà, M. Monno

# Accepted Manuscript

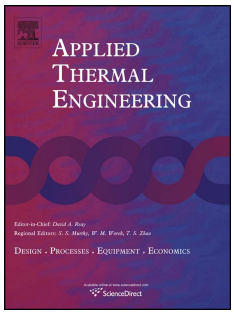


Title: A new approach to the prediction of temperature of the workpiece of face milling operations of Ti-6Al-4V

Authors: G.M. Pittalà, M. Monno

PII: S1359-4311(10)00370-4

DOI: 10.1016/j.applthermaleng.2010.08.027

Reference: ATE 3220

To appear in: *Applied Thermal Engineering*

Received Date: 22 March 2010

Revised Date: 26 August 2010

Accepted Date: 29 August 2010

Please cite this article as: G.M. Pittalà, M. Monno. A new approach to the prediction of temperature of the workpiece of face milling operations of Ti-6Al-4V, Applied Thermal Engineering (2010), doi: 10.1016/j.applthermaleng.2010.08.027

Title: **A new approach to the prediction of temperature of the workpiece of face milling operations of Ti-6Al-4V.**

Authors: G.M. Pittalà, M. Monno

*Department of Mechanical Engineering, Politecnico di Milano, Via La Masa 1, 20156, Milano, Italy*

Phone: +390523623190

Fax: +390523645268.

E-mail address: gaetano.pittala@polimi.it (G. M. Pittalà)

Abstract:

The machining of titanium alloys is critical because of high temperature reached at the tool nose, the segmentation of chip that causes chipping of the tool. The strategy used in the job shop is to use low cutting speed (50-70 *m/min*) and high feed rate (0.1-0.2 *mm/tooth*) in flooding condition in order to reduce the tool temperature and avoiding chipping. The edge preparation and the coating play an important role from thermal point of view. In particular a right compromise between sharp edge and the needs of the coating has to be taken into account.

A reliable thermal model of cutting process of titanium alloy is useful in order to design the cutting edge, calculate the optimal quantity of coolant, and analyze the effect of the coatings.

In this paper a new methodology to the temperature prediction of milling is proposed. The temperature of the workpiece, during the milling operation, has been measured using infrared camera. During the experiments cutting speed and feed rate have been changed. After data analysis a FEM model of cutting process during milling has been developed. The rheological model is calibrated using different milling tests. The results of the model have been compared with the experimental data, obtaining a good agreement. The approach can be useful to the insert tool designer in order to improve the cutting tool performance.

Keywords: FEM, temperature, milling.

## *1. Introduction*

Titanium and its alloys are lightweight, corrosion resistant and high temperature materials. Titanium has the highest strength-to-weight ratio of all commonly used metals up to 550 °C. Titanium and its alloys are used extensively in aerospace because of their excellent combination of high specific strength, which is maintained at elevated temperature, their fracture resistant characteristics, and their exceptional resistance to corrosion. Titanium milling is widely used in the aerospace industry, i.e. pocket realization, and are also used increasingly in other industrial and commercial applications, such as military, racing and medical.

The machining of Ti is critical because of high temperature in a small, concentrated area at the tool tip and the segmented chip formation with adiabatic shear band due to mechanical instability. The high tool temperature produces tool diffusion wear and limits the cutting speed. The chip shear band formation creates the fluctuation in cutting forces and the associated chipping at tool cutting edges. Ti machining has been studied extensively in the past as reported in Ezugwu and Wang [1].

An important effect of temperature is on the tool wear. It is generally known that the progressive tool wear is produced by temperature dependent mechanism as explained in Wanigarathne et al. [2]. Many researchers have worked on temperature measurement and prediction. A review of some experimental measurement can be found in Komanduri and Hou [3].

Davies et al. [4] used the pyrometers and Dewes et al. [5] has analyzed the machining of hardened mould/die steel.

Brandao et al. [6] presents an experimental and theoretical study on heat flow when end milling hardened steels at high-speed. The temperatures on the workpiece have been measured. The heat transferred to the workpiece and the average convection coefficient for the cooling system have been evaluated in order to minimize the error between theoretical and experimental results.

Ceretti et al. [7] have determined the global heat coefficient as function of the local pressure and temperature at the tool-workpiece interface. The global heat coefficient is determined by an iterative procedure, until the error between the theoretical and the experimental temperature is negligible.

Dinc et al. [8] have been performed a validation of finite difference temperature model considering the temperature measured by a high precision infrared camera.

Grzesik [9] has used a standard K-type thermocouple embedded in the workpiece.

Lin [10] has studied the end milling operation of AISI 1050, and Al 6061-T6. The temperature was measured by an infrared (IR) pyrometer. The predictions were performed using the finite element method, that was calibrated by an inverse method.

Ming et al. [11] have measured the temperature on the workpiece by infrared thermometer and the tool temperature by thermocouple, during high speed milling aluminum alloy.

M'Saoubi and Chandrasekran [12] investigated the effects of tool micro-geometry and coating on tool temperature during orthogonal turning of quenched and tempered steel.

Abukhshim et al. [13] presents the measurement of temperature by a thermal imaging camera when high speed cutting of high strength alloy.

A two-color pyrometer with a chalcogenide opical fiber was used from Ueda et al. [14] in order to measure the temperature on the flank face of a cutting tool in high speed milling of AISI 1045.

Filice et al. [15] have measured the tool temperature by a thermocouple based approach and a thermographic analysis.

Radio radiation (two color) thermometry was used from Lazoglu et al. [16].

The measurement of temperature in the machining of titanium was performed from Hong and Ding [17] by embedded thermocouple technique, from Muller et al. [18] by a two-color pyrometer with high spatial and temporal resolution, and from Kitigawa et al. [19] by the tool-work thermocouple.

The prediction of the performance of cutting process and the influence of the process parameters on the product quality is important for tool and process design.

The prediction of temperature remains challenging due to the complexity of the contact phenomena in the metal cutting process as explained in Abukhshim et al. [20].

Yvonnet et al. [21] have determined the heat flux flowing into the tool through the rake face and the heat transfer coefficient between the tool and the environment during a typical orthogonal cutting process. The followed approach is based on an inverse method.

Richardson et al. [22] have predicted the temperature in dry milling using an analytical approach, considering the analytical moving heat source method.

In this paper the simulation of temperature field of the workpiece during face milling of Ti6Al4V using DEFORM$^{TM}$-2D and DEFORM$^{TM}$-3D has been performed. The rheological model has been calibrated on the basis of milling tests. Finally a sensitivity analyses about the material model is carried out in order to know their effect on the solution. The results have been compared with the experimental temperatures, measured by an infrared thermal imager.

## 2. *Experimental set up*

The tests are carried out on four-axis milling centre.

A Mitsubishi cutter body, APX3000R284WA25SA, is used to hold four inserts. The diameter $D_c$ is 28 *mm*. The coated WC-Co tool insert, Mitsubishi AOMT123620PEER-M with 2 *mm* nose radius,

honed cutting edge, and VP15TF grade material (a PVD thin (Al,Ti)N coating) is used in this study. The rake angle is 0° and the relief angle is 11°. The edge radius is 0.05 mm.

The three components of the cutting forces on the workpiece are measured by Kistler 9255B 3-axis piezoelectric dynamometer. The force signals were processed using the charge amplifiers and recorded by a PC-based data acquisition system.

The temperature has been measured using an infrared thermal imager FLIR ThermaCAM SC3000, a long wave, self-cooling analysis system with a cool down time of < 6 min. It has a temperature range of -2' to +2000 °C with an accuracy ±2% or 2°C for measurement above 150°C. This camera can acquire images and data at high rates of up to 750 Hz PAL/900 Hz NTSC with ThermaCAM ResearcherTM HS package. The emissivity of the workpiece material was evaluated matching the temperature with a known temperature.

The ThermaCAM SC3000 is positioned as indicated in the Fig. 1. The camera was positioned at a distance of 30 *cm* from the tool workpiece and it is inside a protective box in order to avoid any damage by the chips, as shown in the Fig. 2.

The milling experiments were performed dry. The cutting speeds ($v_c$) were 35 and 70 *m/min* and the feed rates ($f_z$) were 0.05 and 0.1 *mm/tooth*. The depth of cut ($a_p$) is 2 *mm*. The length of cut is 50 *mm*. The cutting conditions are summarized in the Table 1.

**Table 1 – Design of milling tests using the thermocamera.**

| ***Test*** | $v_c$ **(m/min)** | $f_z$ **(mm/tooth)** | $a_p$ **(mm)** |
|---|---|---|---|
| 1 | 35 | 0.05 | 2 |
| 2 | 35 | 0.1 | 2 |
| 3 | 70 | 0.05 | 2 |
| 4 | 70 | 0.1 | 2 |

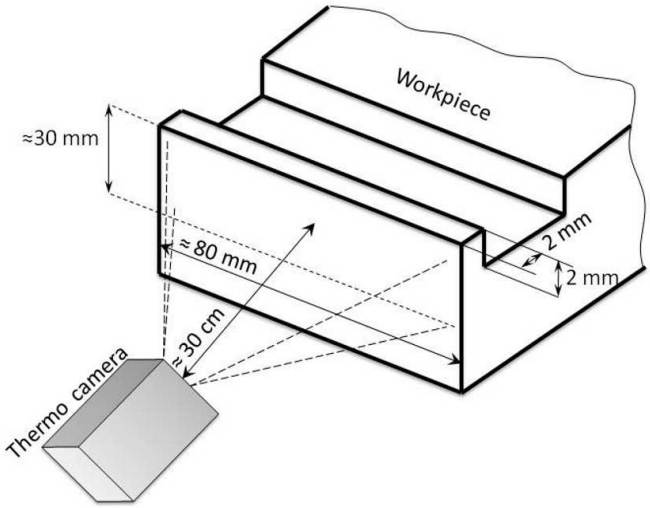


**Fig. 1 – Schema of the experimental set up.**

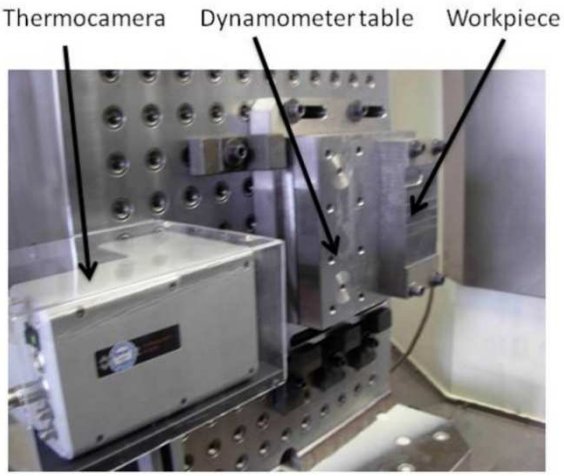


**Fig. 2 – Image of the experimental set up**

## *3. Rheological model and friction set up*

In this section the rheological model set up is presented. The theoretical background, design of milling experiments and the results are explained.

### 3.1 Approach

An analytical-based computer program called OXCUT [23], developed at the Engineering Research Center for Net Shape Manufacturing at the Ohio State University, has been used to obtain flow stress parameters. It is based on Oxley machining theory, and compares the experimental data with the predictions and minimize the error by adjusting flow stress parameters. The program stops its calculation if the results match within a certain, predefined tolerance. In particular a modified Johnson Cook (Eq. 1) has been used for the calibration.

$$\sigma = (A + B\varepsilon^n)\left(1 + C\ln\left(\frac{\dot{\varepsilon}}{\dot{\varepsilon}_0}\right)\right)\left(1 - \left(\frac{T - T_{room}}{T_{melt} - T_{room}}\right)^m\right) \quad (1)$$

with $A = 0$.

The use of these constitutive equations is for reducing the problem of non-uniqueness.

The first term of modified *J-C* equations which represents strain hardening behavior of the material is consisted of parameter *B* and *n*, namely strength coefficient and strain hardening. The initial stress parameter *A* is disregarded due to no initial stress assumption addressed in Oxley's theory and that small number of parameters are preferred for reducing the less computational time and obtaining uniqueness of the solution. The second term which represents the effect of strain rate is assumed to be similar to that of Johnson & Cook's model.

The third term is the temperature factor defined differently for different materials.

The criterion used in matching the predictions and the measurements is the total of the least mean square error between predicted force and measured forces at each rotation angle, and the weighted error of deformation zone ratio at *90th* degree rotation angle between experiments and predictions.

The error function is summarized in the equations (2). From the equation, *f* function refers to the nonlinear function representing Oxley's theory with arbitrary flow stress parameter inputs (*B*, *C*, *n*, and *m*) for predicting forces, deformation, etc. Weighted constants for the error of deformation zone ratios are set as 1000 for $W_1$ and 2000 for $W_2$ since they give less computational time during minimization of the error.

Minimize $\sum_i (RMS\ Error\ forces + Error\ R_p\ and\ R_s)_i = f(B, c, n, m)$

$$\sum_i \left( \sqrt{\sum_\theta \left\{ \left(F_{c,exp}(\theta) - F_{c,the}(\theta)\right)^2 + \left(F_{f,exp}(\theta) - F_{f,the}(\theta)\right)^2 \right\}} + \left( W_1 \left| R_{p,exp}\left(\frac{\pi}{2}\right) - R_{p,the}\left(\frac{\pi}{2}\right) \right| + W_2 \left| R_{s,exp}\left(\frac{\pi}{2}\right) - R_{s,the}\left(\frac{\pi}{2}\right) \right| \right) \right)_i = f(B, c, n, m)$$

(2)

Where:

$F_c$ = Tangential force.

$F_f$ = Radial force.

$R_p$ = Primary deformation zone ratio ($\Delta s/l$).

$R_s$ = Secondary deformation plastic zone ratio.

$W_1$ = Weighted Constant for the error of $R_p$.

$W_2$ = Weighted Constant for the error of $R_s$ ($s/t_{ch}$).

$l$ = Number of cutting conditions .

The symbols are shown in the Fig. 3.

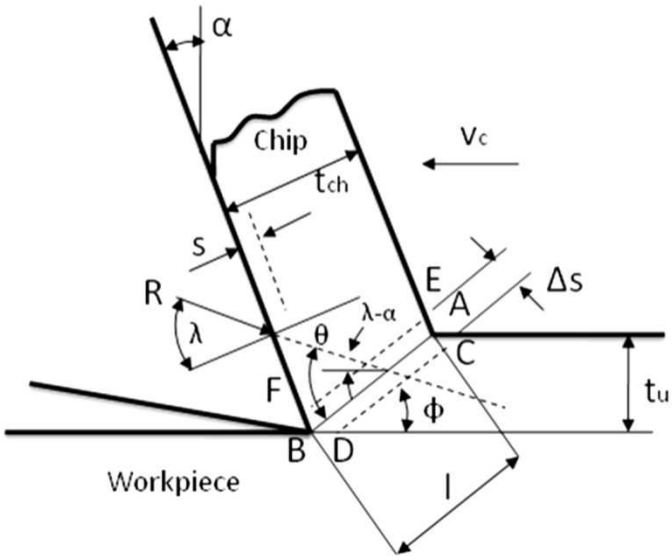


**Fig. 3 - Parallel sided shear zone model**

Downhill simplex [24], a minimization method for multidimensional problem, is used to minimize the error between predictions and measurement by tuning the flow stress parameters and iterating until the error reaches a minimum. Required inputs for Downhill simplex method are the initial guess and minimum tolerances (0.001 as default).

The program was extensively used in the orthogonal cutting and orthogonal slot milling. Pittalà and Monno [25] have used it in the face milling of aluminum.

The thickness of secondary plastic zone is difficult to measure. A theoretical approach has been followed in this paper.

The thickness of the shear zone $\Delta s$ changes little with speed but a great deal with undeformed chip thickness (Oxley [26]).

AB is assumed to be a direction of maximum shear strain rate and it is given by:

$$\dot{\gamma}_{AB} = C\frac{V_S}{l} \tag{3}$$

For the parallel-sided shear zone theory the shear strain-rate is assumed to be constant throughout the shear zone and to be given:

$$\dot{\gamma}_{AB} = \frac{V_S}{\Delta s} \tag{4}$$

Where $V_S$ is the shear velocity. Then $R_p = \Delta s/l = 1/C$.

In general $\Delta s/l$ can be considered constant for usual cutting conditions. In the parallel-sided shear zone theory $C$ = 10. Finally $C$ is 10 and $R_s$ is 0.05.

### 3.2 Experimental set up

The milling tests, performed in order to set up the material model, are different from those where the temperature has been measured. The workpiece is made of the same material and has the shape indicated in the Fig. 4. The milling tool is a Mitsubishi VC-MHDRB 22XR1.5X20; it has four teeth and the diameter is 22 *mm*.

The depth of cut is maintained constant to 2.3 mm. The cutting speed assumes two values (40 and 70 m/min), in order to have different values of the strain rate in the shear plane.

The design of experiment is indicated in the Table 2.

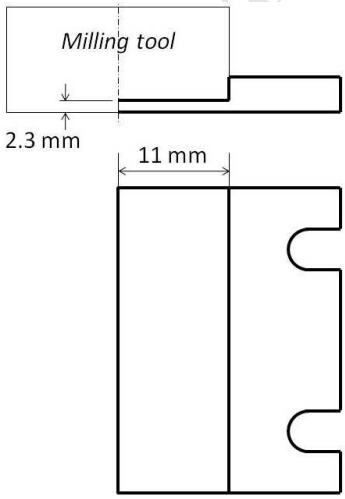


**Fig. 4 – Draw of the workpiece used to set up of the material model.**

**Table 2 – Design of experiments for the rheological model setup**

| Cutting speed (m/min) | Feedrate (mm/tooth) |
|---|---|
| 40 | 0.05 |
| 40 | 0.1 |
| 70 | 0.05 |
| 70 | 0.1 |

The cutting forces on the workpiece are measured by Kistler 9255B 3-axis piezoelectric dynamometer. The force signal was processed using the charge amplifiers and recorded by a PC-based data acquisition system.

### 3.3 Results

The results of OXCUT software are shown in the Table 3:

**Table 3 - Flow Stress Parameters of the simplified Johnson-Cook model**

| *B (MPa)* | *C* | *n* | *m* |
|---|---|---|---|
| 1508 | 0.067 | 0.049 | 0.71 |

The ranges of validity are:

1. Strain = 0.65 to 0.71.
2. Strain rate = $2.2 \cdot 10^{4}\ s^{-1}$ to $1.7 \cdot 10^{5}\ s^{-1}$;
3. Temperature = 374 °*C* to 1129 °*C*.

Different material models have been used in order to analyze their influence on the predicted temperature. They are shown in the Table 4.

**Table 4. Material models**

| **Source** | | **A (MPa)** | **B (MPa)** | **C** | **n** | **m** | $\dot{\varepsilon}_0$ | **Method** |
|---|---|---|---|---|---|---|---|---|
| Lee and Lin [27] | M1 | 782.7 | 498.4 | 0.028 | 0.28 | 1.0 | $10^{-5}$ | SHPB |
| Meyer and Kleponis [28] | M2 | 896 | 656 | 0.0128 | 0.5 | 0.8 | 1 | SHPB |
| Dumitrescu et al. [29] | M3 | 870 | 990 | 0.008 | 1.01 | 1.4 | 1 | Orthogonal cutting |
| Ozel and Karpat [30] | M4 | 987.8 | 761.5 | 0.01516 | 0.41433 | 1.516 | 2000 | Orthogonal cutting |
| New | M5 | 0 | 1508 | 0.067 | 0.049 | 0.71 | 1000 | Milling |

Regard to the M2, M3 and M4 the Cockcroft&Latham damage model has been used. The *D* values for M2 and M3 have been obtained from Umbrello [31]. These are *D*=200 *MPa*, 100 *MPa*, 100 *MPa* respectively. Some sensibility analyses have shown that the mean value of the cutting forces and the workpiece temperature are not significantly influenced from the *D* parameter.

The friction model used is the shear constant model. The friction coefficient is assumed *m* = 0.70-0.80, based on previous face milling tests, using single tooth milling tool (Pittalà [32]).

## 4. FEM Model

The milling operation has been split in several angular steps (Fig. 5) and a 2D FEM simulation for each step has been executed.

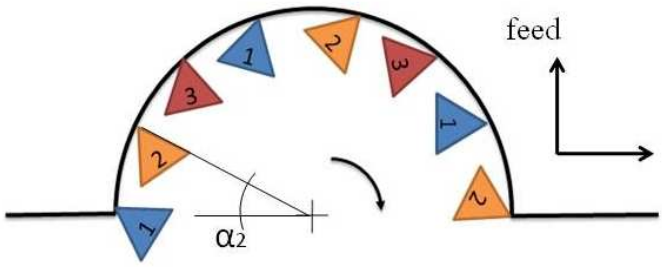


**Fig. 5 - Different positions of milling tool with the inserts n. 1, n. 2, n. 3**

In this way the cutting forces are tangential and radial, or fixed to the tool reference. With the known equations, the feed and perpendicular to feed components, for each insert *i*, can be obtained.

$$F_{feed,i} = b \cdot \left[F_c \cdot cos\alpha_i + F_f \cdot sin\alpha_i\right] \quad (5)$$ , along the feed rate direction.

$$F_{perp-feed,i} = b \cdot \left[F_c \cdot sin\alpha_i - F_f \cdot cos\alpha_i\right] \quad (6)$$, normal to the feed rate direction.

Where $\alpha_i$ is the rotation angle of the insert *i*.

The total force can be obtained with the equation:

$$F_{feed} = \sum_{i=1}^{z} F_{feed,i} \quad (7)$$

$$F_{perp-feed} = \sum_{i=1}^{z} F_{perp-feed,i} \quad (8)$$

$$F_{res} = \sqrt{F_{feed}{}^2 + F_{perp-feed}{}^2}, \quad (9)$$, the total resultant cutting force.

With *z* number of inserts.

The commercial FEA software Deform™-2D v. 9.0, a lagrangian implicit solutor, was used to simulate the operation. The workpiece has 1500 elements, and the tool has 700 elements.

The tool is considered a rigid body and the material is WC.

The FEM permits to obtain the relation between cutting forces and chip thickness for different cutting speed and feedrates.

$$F_c/b = K_{ts} \cdot t_u + K_{te} \quad (10)$$

$$F_f/b = K_{fs} \cdot t_u + K_{fe} \quad (11)$$

The geometry of cutting tool in proximity of the cutting zone, has been modeled as in the Fig. 6.

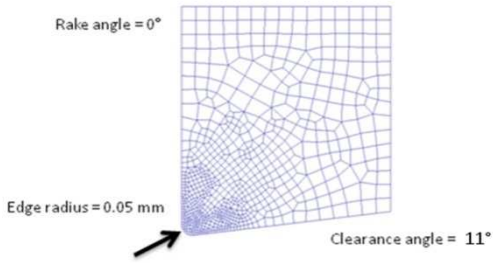


**Fig. 6 - Schematic diagram of the tool**

The depth of cut is increased to the value 3.14 *mm*, to take into account the nose radius.

The boundary conditions are presented in the Fig. 7.

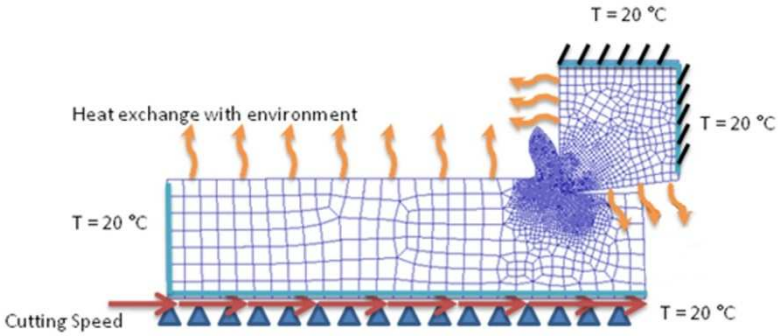


**Fig. 7 - Scheme of boundary condition of 2D FEM model.**

The thermal characteristics of WC is listed in the Table 5:

**Table 5. Thermal characteristics of WC used in the simulation**

| *Conductivity* $(W/(m \cdot °C))$ | *Heat capacity* $(MJ/(m^3 \cdot °C))$ |
|---|---|
| 59 | 15 |

The virtual cutting coefficients have been identified in order to calculate the cutting forces. The results for the material M5 is shown in the Table 6.

**Table 6 – Virtual cutting coefficients for the M5 material**

| Cutting speed (*m/min*) | $K_{cs}$ $(N/mm^2)$ | $K_{te}$ $(N/mm)$ | $K_{st}$ $(N/mm)$ | $K_{se}$ $(N/mm)$ |
|---|---|---|---|---|
| 40 | 1700 | 30 | 570 | 60 |
| 70 | 1600 | 30 | 600 | 60 |

## *5. Thermal model*

The thermal characteristics of titanium is shown in the Table 7.

**Table 7. Thermal data of titanium alloy – TiAl6V4 (Deform-User Manual [33])**

| Heat capacity (x$10^6$ $J/(m^3K)$) | Conductivity $(W/(m \cdot K))$ |
|---|---|
| 2.35 (0 °C) | 7 (0 °C) |
| 2.52 (200 °C) | 8.6 (200 °C) |
| 2.76 (400 °C) | 11.5 (400 °C) |
| 3.5 (600 °C) | 14.4 (600 °C) |
| 3.9 (800 °C) | 17.2 (800 °C) |

The 3D model of the workpiece has been prepared, and the boundary conditions are shown in the Fig. 8 a). It is assumed that the thermal contact between the tool and the workpiece is not intermittent, since there is enough time to evacuate the heat generated from cutting process. The temperature on the arc of contact is obtained from 2D simulation, as presented in the Fig. 8 b). The interface heat coefficient between tool and chip was assumed 10000 *N/s/mm/°C*, considering the thermal contact perfect. As shown in the Fig. 8 b) the thermal gradient on the workpiece is high. It is assumed that the mean value of temperature over a region, indicated in the figure, governs the heat flux.

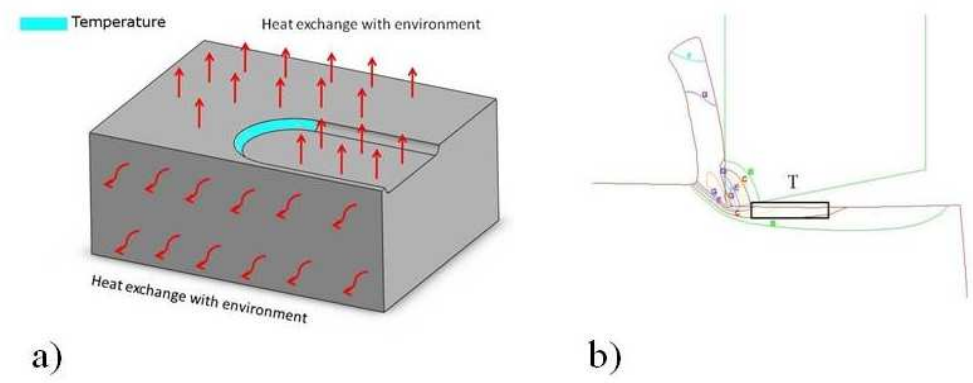


**Fig. 8 - Boundary conditions of the thermal model a) and the temperature of the 2D FEM b).**

The temperature along the depth of cut is assumed constant. Several 2D simulations have been performed in order to take into account the chip thicknesses from zero to the maximum chip thickness.

A sensitivity analysis was performed in order to estimate the influence of the discretization of thermal boundary condition. It was tested: 1) 2 chip thicknesses 2) 3 chip thicknesses, 3) 5 chip thicknesses and 4) 2 chip thicknesses with no temperature at the initial and exit phase.

The four thermal profiles are shown in the Fig. 9.

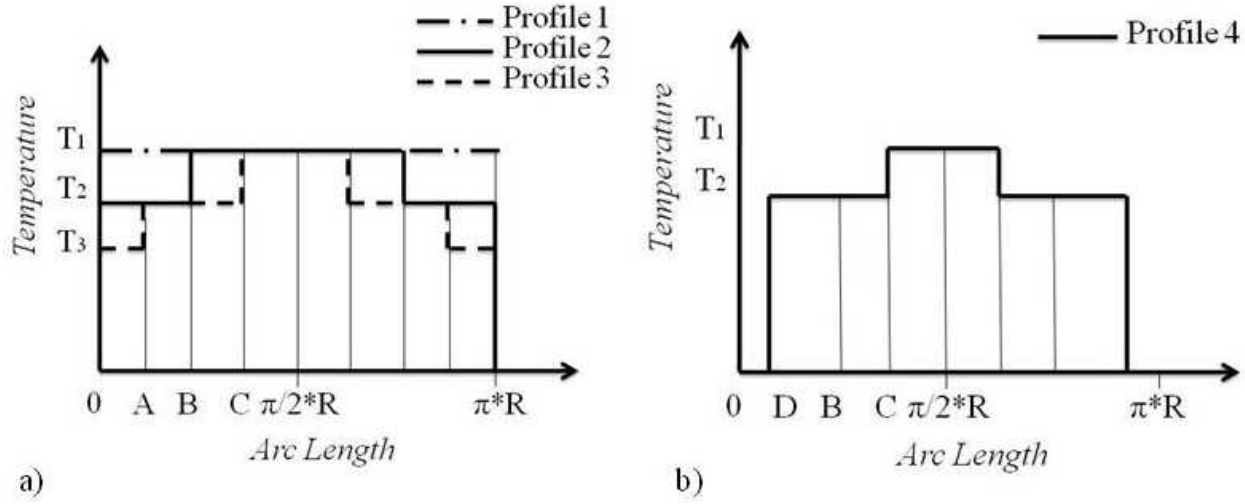


**Fig. 9 - Different thermal profiles**

The chip thicknesses referred to the positions *A*, *B*, *C* and *D* are obtained from the formula $f_z \cdot sen(\alpha)$, with $f_z$ the feedrate in mm/tooth and $\alpha$ the rotation angle. The values are shown in the Table 8.

**Table 8 – Values of the chip thickness of the different positions.**

| Position | Rotation angle (degree) | Chip thickness |
|---|---|---|
| A | 22.5 | $0.382 \cdot f_z$ |
| B | 45 | $0.707 \cdot f_z$ |
| C | 67.5 | $0.923 \cdot f_z$ |
| D | 10 | $0.174 \cdot f_z$ |

The temperature was estimated with 2D FEM simulation.

In this case $f_z = 0.1\ mm/tooth$, and the cutting velocity is 35 *m/min*. The material model is the M5 model

The results are presented in the Fig. 10.

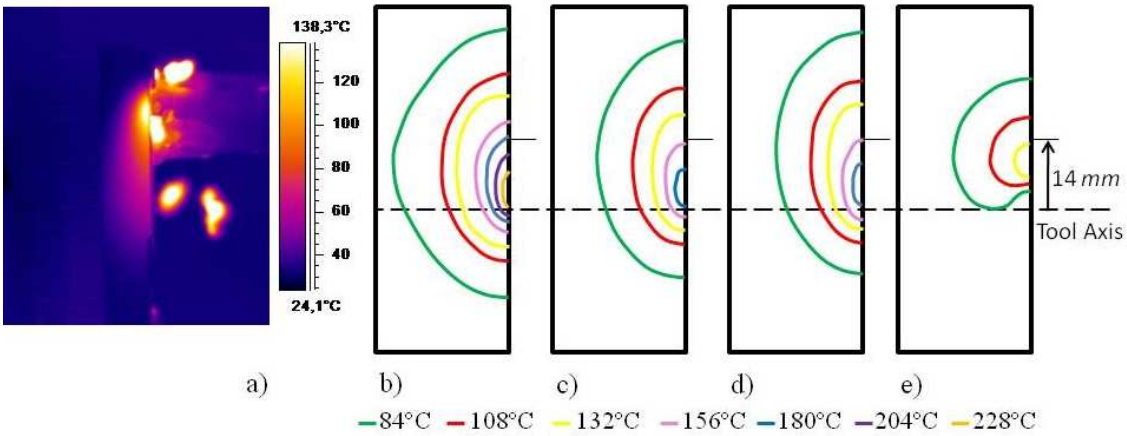


**Fig. 10 – Experimental measurement for the temperature a) and simulation results for different thermal profiles 1 b), 2 in c), 3 in d), 4 in e)**

The thermal profile 2 and 3 give the same result. Subsequently only the profile n. 2 will be considered. It is interesting to note that it is important the thermal conditions for the low chip thickness. If this is neglected, the maximum temperature is underestimated, as shown the Fig. 10 *e*).

Deserves consideration apart the effect of the cobalt content and coating. Some sensibility analysis have been performed. The thermal properties have been taken from the software DEFORM 2D$^{TM}$. In the study 24%, 19% and 15% of cobalt content and the coating TiAlN (thickness 5 µm) have been taken into account.

The results show that the temperature of the workpiece changes around 5-6%. A considerable difference, of course, can be found for the maximum temperature of the cutting tool.

Finally, the experimental determination of thermal properties of the coating and cutting tool in the state of cutting process need further study. The determination of the thermal conductivity and thermal capacity of tungsten carbide with different cobalt content and coating is not the object of this paper. Anyway the sensitivity analysis shows that the effect on the temperature workpiece is not very remarkable.

## *6. Results*

In this section the results in terms of the mean values of the cutting forces and the maximum temperature reached on the workpiece have been taken into account.

In the Fig. 11 the resultant cutting forces on the cutting plane is shown. In the figure is also shown the experimental error (the dotted line).

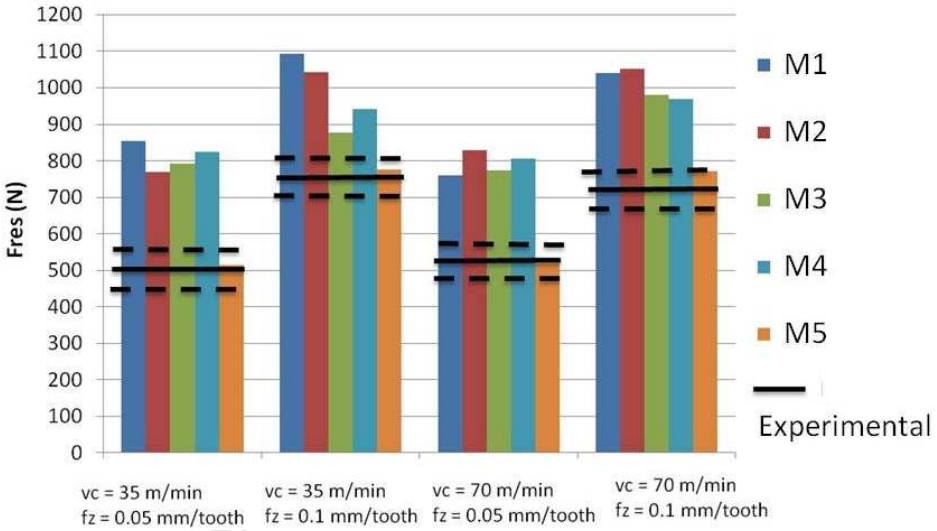


**Fig. 11 – Mean value of the resultant cutting forces on the cutting plane changing the cutting conditions.**

It can be noted that for the material models M1, M2, M3, M4 the cutting forces are overestimated for all the cutting conditions. The M5 provides a good agreement with the experimental results.

The maximum temperature on the workpiece (where the temperature has been measured) is presented in the Fig. 12 (the dotted line indicates the experimental error).

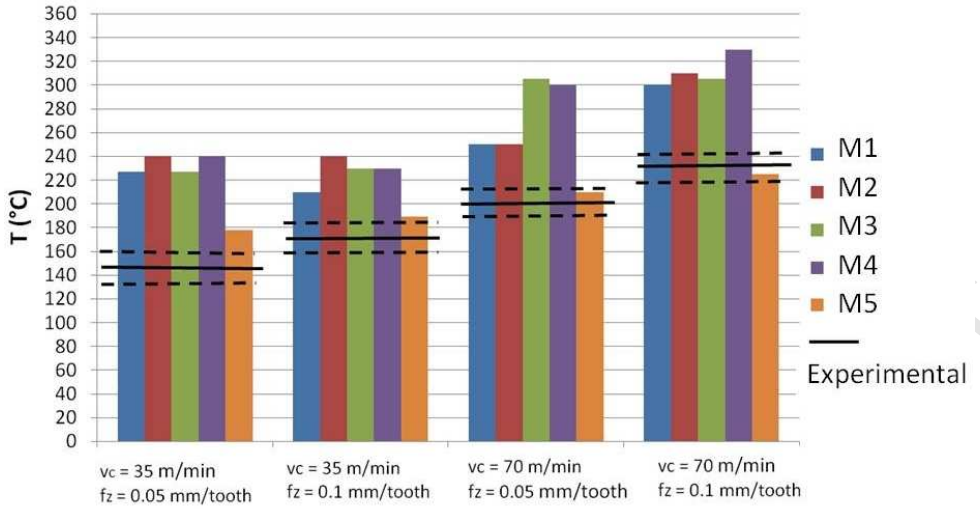


**Fig. 12 – Maximum temperature on the workpiece changing the cutting conditions for different material models.**

The M5 model is, among all models, one that provides the best agreement between theoretical results and experimental ones.

## *7. Conclusions*

In this paper the thermal prediction of Ti6Al4V milling has been considered. Face milling tests were carried out on a milling centre using a milling tool with four inserts.

A methodology was set up in order to predict the temperature of the workpiece due to the face milling. The approach is based on the *2D* FEM in order to estimate the thermal field due to the cutting process, and thermal simulation using *3D* FEM to obtain the temperature on the workpiece. Sensitivity analyses about the boundary conditions of the thermal simulation were performed and the best set up was determined.

The procedure is consistent because it provides a good agreement of theoretical and experimental temperature.

The analysis shows the need to calibrate the material directly from face milling operations. In fact the better agreement, regard to the cutting forces and temperatures, is obtained when the rheological model is derived from milling test.

This work can be useful to estimate the thermal field on the workpiece and then the distortions of its. This is useful to analyze the effect of cutting fluid, and then optimize the flow rate.

**Acknowledgement**
I would like to thank Mr. C. Repetti of DEMA company for providing the tool, the workpiece and the use of milling center, and Mr. F. Cacciatore for the use of thermo camera.

## References

[1]. E.-O. Ezugwu, Z.-M. Wang, Titanium alloys and their machinability – a review, J. Mater. Process. Tech. 68/1 (1997) 262-274.

[2]. P.C. Wanigarathne, A.D. Kardekar, O.W. Dillon, G. Poilachon, I.S. Jawahir, Progressive tool-wear in machining with coated grooved tools and its correlation with cutting temperature, Wear. 259 (2005) 1215-1224.

[3]. R. Komanduri, Z.B. Hou, A review of the experimental techniques for the measurement of heat and temperatures generated in some manufacturing processes and tribology, Tribol. Int. 34 (2001) 653-682.

[4]. M.A. Davies, Q. Cao, A.L. Cooke, R. Ivester, On the measurement and prediction of temperature fields in machining AISI 1045 steel, Annals of CIRP. 52/1 (2003) 77-80.

[5]. R.C. Dewes, E. Ng, P.G. Newton, D.K. Aspinwall, Temperature measurement when high speed machining hardened mould/die steel, J. of Mat. Process. Technology. 92-93 (1999) 293-301.

[6]. L.C. Brandao, R.T. Coelho, A.R. Rodrigues, Experimental and theoretical study of workpiece temperature when end milling hardened steels using (TiAl)N-coated and PcBN-tipped tools, J. of Mat. Process. Tech. 199 (2008) 234-244.

[7]. E. Ceretti, L. Filice, D. Umbrello, F. Micari, ALE Simulation of Orthogonal Cutting: a New Approach to Model Heat Transfer Phenomena at the Tool-Chip Interface, Annals of the CIRP. 56 (2007) 69-72.

[8]. C. Dinc, I. Lazoglu, A. Serpenguzel, Analysis of thermal fields in orthogonal machining with infrared imaging, J. of Mat. Process. Tech. 198 (2008) 147-154.

[9]. W. Grzesik, Experimental investigation of the cutting temperature when turning with coated indexable inserts, J. Mach. Tools Manufacture. 39/3 (1999) 355-369.

[10]. J. Lin, Inverse estimation of the tool-work interface temperature in end milling, Int. J. Mach. Tools. Manufact. 35/5 (1995) 751-760.

[11]. C. Ming, S. Fanghong, W. Haili, Y. Renwei, Q. Zhenghong, Z. Shuqiao, Experimental research on the dynamic characteristics of the cutting temperature in the process of high-speed milling, Journal of Materials Processing Technology. 138 (2003) 468-471.

[12]. R. M'Saoubi, H. Chandrasekaran, Investigation of the effects of tool micro-geometry and coating on tool temperature during orthogonal turning of quenched and tempered steel, International Journal of Machine Tool & Manufacture. 44 (2004) 213-224.

[13]. N.A. Abukhshim, P.T. Mativenga, M.A. Sheikh, Heat generation and temperature prediction in metal cutting: A review and implications for high speed machining, Int. J. Mach. Tools. Manufact. 46 (2006) 782-800.

[14]. T. Ueda, A. Hosokowa, K. Oda, K. Yamada, Temperature on flank face of cutting tool in high speed milling, Annals of the CIRP. 50 (2001) 37-40.

[15]. L. Filice, D. Umbrello, S. Beccari, F. Micari, On the FE codes capability for tool temperature calculation in machining processes, J. of Materials Processing Technology. 174 (2006) 286-292.

[16]. I. Lazoglu, K. Buyukhatipoglu, H. Kratz, F. Klocke, Forces and temperatures in hard turning, Machining Science and Technology. 10/2 (2006) 157-179.

[17]. S.Y. Hong, Y. Ding, Cooling approaches and cutting temperatures in cryogenic machining if Ti-6Al-4V, International Journal of Machine Tools and Manufacture. 41 (2001) 1417-1437.

[18]. R.U. Muller, S. Hoppe, F. Klocke, Radiation thermometry at a high-speed turning process, Trans. ASME, Journal of Manufacturing Science and Engineering. 126/3 (2004) 488-495.

[19]. T. Kitigawa, A. Kubo, K. Maekawa, K., Temperature and wear of cutting tools in high-speed machining of Inconel 718 and Ti-6Al-6V-2Sn, Wear. 202 (1997) 142-148.

[20]. N.A. Abukhshim, P.T. Mativenga, M.A. Shiekh, Investigation of heat partition in high sped turning of high strength alloy steel, Int. J. Mach. Tools Manufacture. 45 (2005) 1687-1695.

[21]. J. Yvonnet, D. Umbrello, F. Chinesta, F. Micari, A simple inverse procedure to determine heat flux on the tool in orthogonal cutting, Int. J. of Machine Tools & Manufacture. 46 (2006) 820-827.

[22]. D.J. Richardson, M.A Keavey, F. Dailami, Modelling of cutting induced workpiece temperatures for dry milling, International Journal of Machine Tools & Manufacture. 46 (2006) 1139-1145.

[23]. P. Sartkulvanich, F. Koppka, T. Altan, T., Determination of flow stress for metal cutting simulation-a progress report, Journal of Materials Processing Technology. 146 (2004) 61-71.

[24]. W.H. Press, S.A. Teukolsky, W.T. Vetterling, B.P. Flannery, Numerical Recipes in C-The Art of Scientific Computing, 2nd ed., Cambridge University Press, New York, 1992.

[25]. G.M. Pittalà, M. Monno, 3D finite element modeling of face milling of continuous chip material, Int. J. of Adv. Manuf. Technol. DOI: 10.1007/s00170-009-2235-0 (2009).

[26]. P.L.B. Oxley, Mechanics of Machining, An Analytical approach to Assessing Machinability. Halsted Press, New York, 1989.

[27]. W.-S. Lee, C.-F. Lin, Plastic deformation and fracture behavior of Ti-6Al-4V alloy loaded with high strain rate under various temperatures, Materials Science & Engineering, Vol. A 241/1 (1998) 48-59.

[28]. H.W. Jr. Meyer, D.S. Kleponis, Modeling the high strain rate behavior of titanium undergoing ballistic impact and penetration, International Journal of Impact Engineering. 26/1 (2001) 509–521.

[29]. M. Dumitrescu, M.A. Elbestawi, T.I. El-Wardany, Mist Coolant Applications in High Speed Machining, Kluwer Academic/Plenum Publisher. (2002) 329-339.

[30]. T. Ozel, Y. Karpat, Identification of Constitutive Material Model Parameters for High-Strain Rate Metal Cutting Conditions Using Evolutionary Computational Algorithms, Materials and Manufacturing Processes. 22/5-6 (2007) 659-667.

[31]. D. Umbrello, Finite element simulation of conventional and high speed machining of Ti6Al4V alloy, Journal of Materials Processing Technology. 196 (2008) 79-87.

[32]. G.M. Pittalà, Finite Element of Milling Operations, Ph.D. Thesis. Politecnico di Milano, 2009.

[33]. Deform$^{TM}$-User Manual, SFTC-Deform V9.0.1, Scientific Forming Technologies Corporation Ed., Columbus, OH, USA, 2006.